12th IAP Astrophysics Colloquium, July 1996, Paris, ed. R.Ferlet

THE CHROMATICITY OF MICROLENSING

D. D. SASSELOV
Harvard-Smithsonian Center for Astrophysics, Cambridge, MA 02138, USA; dsasselov@cfa.harvard.edu

Abstract

Gravitational microlensing is not achromatic when the star being microlensed is resolved by the lens. We show how narrow-band photometry and moderate- to high-resolution spectroscopy can be used to reconstruct the stellar surface intensity distribution of a microlensed star. Such microlens imaging can provide a unique opportunity to study the surfaces of normal red giants where Doppler imaging is not applicable due to slow rotation.

1 Introduction

Microlensing events have often been advertised as achromatic, but there are a number of conditions which will introduce a wavelength dependence in the light curves and in spectral features of an observed event. Among them are light from the lens which has a different color from the source [1] and blended sources, where only one star of a blend is likely to be lensed [2, 3]. Here we are interested in a third source of chromaticity – finite-size effects, because these arise from resolved features on the surface of the lensed star. Such effects are observable at a level at which they provide an excellent opportunity for stellar surface imaging [4].

Finite-size effects have been studied as methods to partially remove the degeneracy of microlensing light curves through the alterations of the standard light curve [5, 6, 7, 8, 9], its polarized emission [10], spectral shifts due to stellar rotation [11], and narrow-band photometry in resonance lines [12]. Here we want to put the emphasis on the inverse problem – reconstructing the stellar surface features and probing the stellar atmosphere.

The total flux observed is wavelength dependent through its dependence on $B(r, \theta)$ – the resolved stellar surface intensity distribution, which can vary strongly with wavelength in selected spectral regions (in continua and within spectral lines). The reconstruction of $B(r, \theta)$ distinguishes our approach from the deconvolution of quasar structure from microlensing light curves (see [13]).

2 Probing Stellar Atmospheres

Stellar research is about to experience a dramatic growth, powered by new fundamental data of unprecedented quality. One source is the *HIPPARCOS* satellite with positions and parallaxes; the other source is the development of stellar interferometers and arrays able to resolve surfaces of nearby stars in ways achievable only for the Sun until now.

The Sun offers an instructive example. On one hand, we have measured the solar radius to 0.001%, its luminosity to 0.003% and its surface temperature to about 2K. On the other hand, the solar disk brightness distribution as a function of wavelength has been mapped into the depth distribution of temperature and density, which allows a complete synthesis of the observed solar spectrum [14]. The situation with stars has been confined to very much lower accuracy. The angular diameters of a very small number of stars have been measured presently; the accuracy is about 10% at best [15]. Stellar disk brightness distributions (limb darkening) have been measured only in a handful of stars at the level of a proof-of-concept (directly – [16, 17]; or in binaries – [18]; they cannot be used to build a model atmosphere, as in the case of the Sun. The possible presence of surface features (like solar spots, active regions, etc.) is only inferred spectroscopically. Therefore our understanding of stellar light is implicitly tied to the solar atmosphere model.

This situation is unfortunate for a number of reasons. There has been an increased demand for accurate stellar models from a number of fields. To name a few, much improved color-temperature calibrations are needed for calibrating distance indicators and determination of ages; stellar population syntheses (e.g. for high-z systems) rely critically on the accuracy of current stellar models. Our Sun is not a good zero point for most of these applications.

The advent of large interferometric arrays will go a long way towards solving these problems, but all of these complex and expensive facilities are still on the drawing boards. In the meantime, gravitational microlensing offers an easily accessible, immediate, and inexpensive way to image at least some types of stars. It also offers, by its nature, access to stellar populations (in the Galactic bulge and Magellanic Clouds), which are beyond the reach of any interferometer.

3 Practical considerations & a model for MACHO Alert 95-30

The amplification of a point source by a point mass, M, depends only on their projected separation d , $A(d) = (d^2+2)/(d(d^2+4)^{1/2})$, where d is expressed in units of the angular radius of the Einstein ring of the lens, $\theta_E = ([4GM/c^2][D_{\rm LS}/D_{\rm OL}D_{\rm OS}])^{1/2}$, and $D_{\rm OL}$, $D_{\rm LS}$, and $D_{\rm OS}$ are the distances between the observer, lens and source. The total flux received from an extended source is therefore obtained by integration over its infinitesimal elements,

$$F(t) = \int_0^{\tilde{R}_s} r dr B(r) \int_0^{2\pi} d\theta A(d),$$

where $B(r)$ is the surface brightness profile of the source in the projected polar coordinates (r, θ) around its center. All projected length scales are normalized by the Einstein ring radius. As a result, although gravitational microlensing is achromatic, when the source is resolved, $F(t)$ is wavelength dependent through $B(r)$.

Microlensing events towards the bulge occur when a low-mass star from the disk (the lens at $\mathrm{D_{OL}} \approx 6kpc$) crosses the line-of-sight towards a star from the bulge (the source at $\mathrm{D_{OS}} \approx 8kpc$); typical durations are between weeks and months. While most lenses are point masses, many ($\sim 20\%$) of the sources monitored in the Galactic bulge are red giants and supergiants – their angular radii are *comparable* to the Einstein radius of a sub-solar mass lens (in the range of 50μas). In addition to being resolved by most lenses, the projected disks of bulge giants are large enough to make the probability for a lens transit very high – in fact, at least one such event (MACHO Alert 95-30) was very well observed last summer [19].

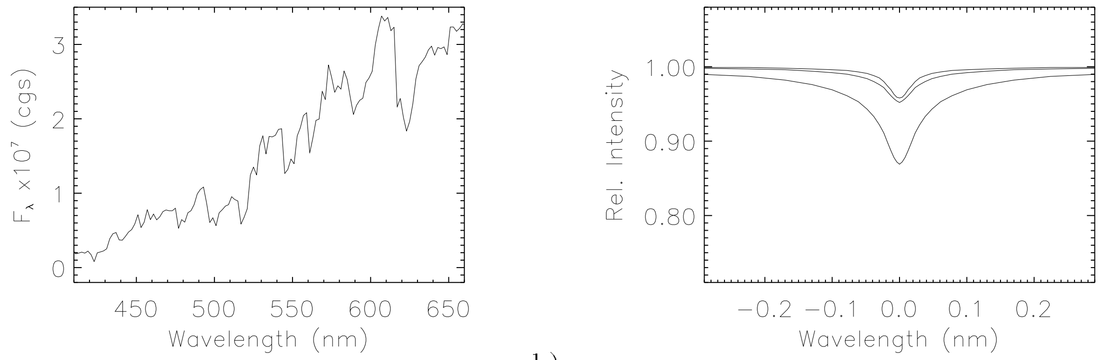

a) b)

Figure 1: The computed optical spectrum for the MACHO 95-30 source. a) The absorption features at 476.2, 495.5, 516.8, 545, 588, & 620 nm are due to TiO. b) Three profiles of the weak hydrogen Hβ line from disk center at μ=0.98 (bottom), through μ=0.5, to very near the limb at μ=0.02 (top).

The conditions for microlens imaging towards the LMC are not as favorable. However, a large number of lenses are binaries (increasingly more are being recognized and observed presently), thus caustic crossings should ensure the necessary resolution. This applies equally to bulge events. In summary, microlens imaging is viable; below we discuss different stellar surface features and the observational requirements for their detection.

As a way to illustrate the opportunities for stellar imaging and the microlensing computer code described here by [20], we will use our model for the red giant which was the source in MACHO Alert 95-30. The giant is best fit with a model atmosphere of $T_{\rm eff}$ = $3500K \pm 200K$, $log\ g$ = 1.0 ± 0.8, and $V_{\rm t}$ = 2 kms^{-1}. The atmosphere is in hydrostatic and radiative equilibrium and has solar (Pop.I) abundances. The opacities are by [21]. This model represents the best fit to the spectrum of MACHO Alert 95-30 obtained by [22] and the available V, R photometry. The model emergent spectrum in the optical is shown in Figure 1a. At least seven TiO bands, CaH and CaI, can be identified well on both the observed and synthesized spectra.

4 Stellar surfaces – center-to-limb variations

4.1 Continuum

Stellar disks are projected hemispheres, which implies an axisymmetric variation of the intensity with position as it maps into a variation with depth. In general, the emergent continuum radiation at the center of the disk is formed deeper than the radiation we see near the limb. Over a very wide spectral range for stars of different temperature, the center-to-limb variation of the contunuum emission is manifested as limb darkening. The amount of limb darkening is a function of wavelength. It has been included in calculations of finite-size effects in microlensing [8, 23].

An example of limb darkening in the V and R passbands and the resulting microlensing light curves is given here in [20]. The curves were calculated for the event MACHO Alert 95-30 with the stellar model described above.

4.2 Spectral lines

Unlike continuum radiation, spectral lines provide a larger choice of center-to-limb variations. In the majority of stars we deal with absorption lines of different strength, arising from atomic or molecular bound-bound transitions. Most moderately strong and weak lines diminish towards the limb (Figure 1b). This variation could be observed in a microlensing event by measuring the total equivalent widths

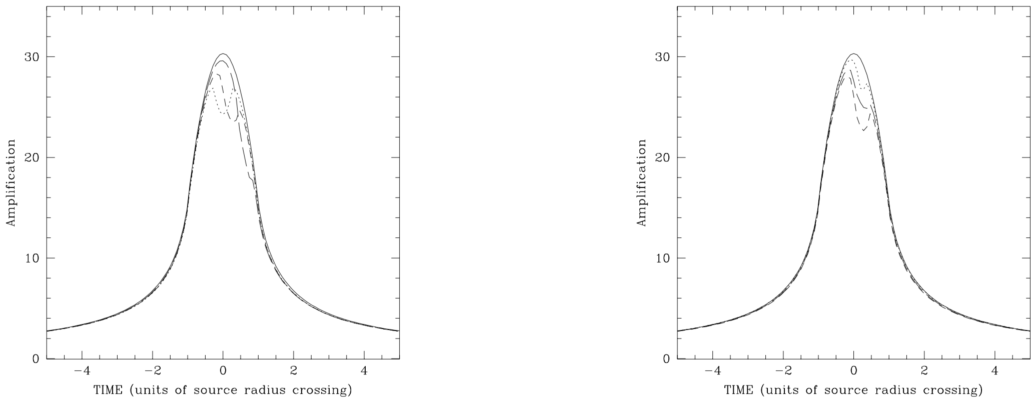

a) b)

Figure 2: Lightcurves for a red giant source with a dark spot. a) Three different positions of a spot with temperature difference (contrast) ΔT=500 K. b) Different spot contrasts: ΔT=250 & 1000 K (dashed); and a twice smaller spot (10% of source radius) at ΔT=500 K (dotted).

of spectral lines on medium-resolution spectra with high S/N. The magnitude of the effect is similar to that of limb darkening, but involves a very narrow range of wavelengths and hence a larger expense in the collection of photons.

Therefore it is advantageous to look for spectral lines which have an exceptionally strong center-to-limb variation. Obviously these will vary by species and by type of star. A good choice would be lines that remain optically thick at the limb and hence appear strongly in emission there. Known as resonant line scattering, this effect is observed in the Sun and should be common to cool stars in spectral lines like Ca II K. The application of resonant line scattering in Ca II to microlensing is discussed in detail by [12], who calculated light curves and showed that it should be possible to observe the effect. In stars of very low surface temperature, like the giant from MACHO Alert 95-30, resonant line scattering may be observed in the optical bands of TiO.

Resonant line scattering is greatly enchanced in the atmospheres of stars which are extended (compared to our Sun) – bright giants and supergiants. So is the effect of limb polarization, discussed here by [24]. Polarimetric measurements, although more difficult, would be a valuable probe of the stellar atmospheres of such stars.

5 Stellar surfaces – spots and other features

Apart from having a venerable history ([25] and references therein), the question of small-scale surface structure in normal stars is very important for stellar modeling. Direct interferometric evidence is scarce and inconclusive [26, 27]. Indirect evidence, such as Doppler imaging and photometry, is limited to specific types of stars. A very complete survey of photometric evidence for stellar spots comes from the OGLE microlensing survey of bulge giants [28].

In [20] we examined the effect of a stellar spot for a range of sizes and contrasts (ΔT) on the microlensing curve observed in an optical passband for an event similar to MACHO Alert 95-30. Spots which are larger than 10% of the radius have strong effect on the light curve, and should be easy to detect (Figure 2). Such spots may be common on red giants and could thus complicate the interpretation of light curves which may be distorted due to a lens companion or planet. To distinguish between spots on the source and companions of the lens, it would be sufficient to have photometry in two or more different spectral bands, as spot contrast is usually wavelength dependent.

To maximize the search for spots and active regions on the surfaces of microlensed stars one should again resort to the use of sensitive spectral lines. Such techniques are widely known and used in the study of the Sun – one example is the bandhead of the CH radical at 430.5 nm, which provides very high contrast to surface structure [29]. This will again require spectroscopy or very narrow-band photometry of the microlensing event, but could be very rewarding. The most practical approach is to microlens the entire synthesized optical spectrum of the source in alerts similar to MACHO 95-30 and look for the most sensitive spectral features in advance of the observations. The code described in [20] is fast enough to allow this for the tens of thousands of frequencies involved.

References

[1] Kamionkowski, M. 1995. *Astrophys. J.* **442**, L9

[2] Alard, C., Mao, S., & Guibert, J. 1995. *Astr. Astrophys.* **300**, 17

[3] DiStefano, R., & Esin, A.A. 1995. *Astrophys. J.* **448**, L1

[4] Sasselov, D.D. 1996. in *Cool Stars 9* eds Pallavicini,R. & Dupree,A.K.,ASP Conf Ser.

[5] Gould, A. 1994. *Astrophys. J.* **421**, L71

[6] Gould, A. 1995. *Astrophys. J.* **441**, 77

[7] Nemiroff, R.J., & Wickramasinghe, W.A.D.T. 1994. *Astrophys. J.* **424**, L21

[8] Witt, H.J., & Mao, S. 1994. *Astrophys. J.* **430**, 505

[9] Gould, A., & Welch, D. 1996. *Astrophys. J.* **464**, 212

[10] Simmons,J.F.L., Newsam,A.M., & Willis,J.P. 1995. *Mon. Not. R. astr. Soc* **276**, 182

[11] Maoz, D., & Gould, A. 1994. *Astrophys. J.* **425**, L67

[12] Loeb, A., & Sasselov, D.D. 1995. *Astrophys. J.* **449**, L33

[13] Grieger, B., Kayser, R., & Schramm, T. 1991. *Astr. Astrophys.* **252**, 508

[14] Kurucz, R.L. 1990. in *Atomic Spectra for Astroph. & Fusion*, p.20, ed Hansen,J.E., North-Holland

[15] Armstrong, J.T. et al. 1995. *Physics Today* **48**, 42

[16] Mozurkewich, D. et al. 1991. *Astron. J.* **101**, 2207

[17] Stee, P. et al. 1995. *Astr. Astrophys.* **300**, 219

[18] Andersen, J. 1991. *A&A Review*, **3**, 91

[19] Pratt, M. 1996. in *2nd Workshop on Grav. Microlensing Surveys* p.243, LAL-Orsay

[20] Heyrovsky,D., Loeb,A., & Sasselov,D. 1996. this volume

[21] Kurucz, R.L. 1992. in *Stellar Population of Galaxies* p.225, ed Barbuy,B.,& Renzini,A., Kluwer

[22] Sahu, K.C. 1996. in *2nd Workshop on Grav. Microlensing Surveys* p.270, LAL-Orsay

[23] Valls-Gabaud, D. 1996. this volume

[24] Coleman,I.J., Simmons,J.F.L., Newsam,A.M. 1996. this volume

[25] Schwarzschild, M. 1975. *Astrophys. J.* **195**, 137

[26] Di Benedetto, G.P., & Bonneau, D. 1990. *Astrophys. J.* **358**, 617

[27] Hummel, C.A. et al. 1994. *Astron. J.* **107**, 1859

[28] Udalski, A. et al. 1995. *Acta Astron.* **45**, 1

[29] Berger, T.E. et al. 1995. *Astrophys. J.* **454**, 531